Three-Dimensional Acoustic Computation of Four-Component Seismic Data

How-Wei Chen[1]

ABSTRACT

The relationships among the (scalar) displacement potential, acoustic pressure and particle displacement is exploited in three-dimensional (3-D) numerical modeling of synthetic multi-component multi-offset seismograms. Using these relations, synthetic one-component pressure and partially resolved three-component (3-C) displacement seismograms may be computed for 3-D models using a finite-difference solution of the (3-D) acoustic wave equation. Compressional- or decoupled-SH and Love wave responses can be used as a complement to elastic response for data interpretation and subsurface structure delineation.

This new capability is applicable to a wide range of recording geometries over various complex structures. Simulations include surface sources recorded on a circular array, walkaway survey, multi-component multi-offset vertical seismic profiling (VSP), and both off-end and off-line shots into a crooked, wide-aperture array. The result indicated that the relationships among source, receiver location and complexity of the subsurface structure will produce different three-component responses. For seismic event identification and subsurface structure discrimination, the uniqueness from forward modeling can be emphasized through integrated approach by considering 3-D scalar, partially resolved 3-C displacement and elastic modeling.

(Key words: 3-D acoustic modeling, Synthetic seismograms, Displacement potential, Four component, Finite-difference)

1. INTRODUCTION

Simulation of wave propagation in complex 2- and 3-D geological media is an important tool to verify geological or geophysical hypotheses by comparing directly the simulated result with the collected data by using either wave theory (Chen & McMechan, 1992; Chen & McMechan, 1993; Chen, 1996) or ray theory (Chen, 1998). Pre-survey design should be evaluated in order to avoid aliasing of the acquired data in time and space. Therefore, computer

---

[1]Institute of Seismology, Institute of Applied Geophysics, National Chung Cheng University, Min-Hsiung, Chia Yi, Taiwan, ROC

simulations of field surveys and testing of the simulated data set for modeling, data processing and analyses are essential. Obvious examples are the Marmousi 2-D (Versteeg and Grau, 1990) and 3-D (Aminzadeh et al., 1995) projects, and the 3-D SEG/EAEG Modeling Project.

To account for the 3-D propagation effects and full wavefield multicomponent marine data recorded by hydrophone and geophone, a 3-D modeling scheme is required. The main advantage is its ability to handle diverse source and arbitrary recording geometries when 3-D effects must be considered. This facilitates modeling reflection or refraction lines which are typically almost linear but require projection to a common line to be processed by 2-D algorithms. An obvious solution is the computation of synthetic seismograms directly in 3-D with variable spacing along a crooked recording line. To simulate 3-D effects commonly observed in field data, a true point source signature and 3-D propagation effects within a spatially varying 3-D velocity distribution are essential. Some parsimonious approaches, such as assuming a spatially varying 2-D medium with modified 3-D source signature and propagating wavefield effects to account for the fundamental difference in amplitude behavior, may not be necessary.

SH and Love waves, i.e., the transverse component of a three-component wavefield, are functionally equivalent to the full acoustic response. The governing equation for decoupled horizontal shear displacement and acoustic wave equation is the same with different physical parameters involved. The similarity between acoustic and SH wave propagation is that the velocity of the sound α can be replaced by the shear wave velocity β, and the elastic parameter μ can also be replaced by the reciprocal of density ρ^{-1}. Love waves are physically the result of the superposition of closely spaced, multiple free-surface post-critical SH reflections (cf. Kelly, 1983). Wide-aperture SH wavefields contain direct waves, pre- and post-critical reflections, wide-aperture refractions, triplications, internal multiples, and Love waves. Therefore, 3-D acoustic computation may become a valuable tool to predict SH components of earthquake data.

Acoustic computation also provides an efficient tool for seismic exploration. Large-scale seismic acquisition experiments, which include joint land and marine-based reflection and refraction surveys, have been proposed in the Republic of China (Taiwan) since 1991. The TAICRUST deep seismic imaging program attempts to apply various state-of-the-art imaging techniques for delineating the subduction-collision tectonic features beneath Taiwan. Similar experiments have been successfully applied in imaging the deep crust along passive and active plate margins and in the continental lithosphere in North America, Europe and Australia. Representative programs are: COCORP, EDGE, and IRIS (U.S.), ECORS (France), DEKORP (Germany), BIRPS (England), Lithoprobe (Canada), and ACORP (Australia). With an appropriate survey configuration, joint sea-land measurements may be suitable for imaging intra- and inter-plate boundaries in both 2-D and 3-D.

Modeling of seismic elastic responses is computationally more complicated than acoustic calculation. Much less computer memory and far fewer arithmetical operations are required for acoustic calculation than for elastic computation for a 3-D problem. Therefore with limited computational resources, the frequency contents of the calculated responses can become higher than the desired elastic computation especially for large-scale seismic simulation.

This work is part of the project conducted over the last five years in Taiwan for developing a wavefield simulation and prestack seismic data processing system for geophysical sur-

veys. In the TAICRUST project, a combined survey including wide angle ocean bottom seismographs (OBS) and multi-channel seismic (MCS) survey was conducted offshore from eastern Taiwan. Four-component (4-C) OBS data, including pressure sensitive hydrophone and three-component velocity sensitive geophone records, were deployed and collected by R/V Ocean Researcher I. The main objective of this paper is to demonstrate the development of a wave-equation based 3-D full acoustic wavefield seismic data simulation system for multi-component seismic data. The proposed scheme can be used as a complement to elastic forward modeling for data interpretation and subsurface structure delineation.

2. THEORY

An algorithm based on the scalar wave equation for generating scalar (hydrophone) and three-component displacement (geophone) seismograms for crooked 3-D seismic survey lines is discussed in the following sections. The primary principle uses the relationships among the (scalar) displacement potential, acoustic pressure, and particle displacement. The approach have not been previously exploited in 3-D numerical modeling of 4-C seismograms probably because modeling of field data has become feasible.

To obtain synthetic three-component displacement (vector U) seismograms for any point in an acoustic medium, as a function of time (t), we may use the properties of the acoustic (scalar) potential (ϕ). By definition (Sheriff and Geldart, 1982; Aki and Richards, 1980; Ewing et al., 1957),

$$U = grad\phi. \tag{1}$$

Thus, if we have potential ϕ at the receiver locations in the medium at all times, we may compute the corresponding three orthogonal components of displacement U (U_x, U_y, U_z) in the x, y and z directions at these locations, at any time t by using equation 1 explicitly as

$$U_x(t) = \partial\phi(t)/\partial x, \ U_y(t) = \partial\phi(t)/\partial y, \text{ and } U_z(t) = \partial\phi(t)/\partial z.$$

The key implementation of equation 1 is to use the scalar wave equation to propagate the displacement potential ϕ, rather than the pressure P. Both P and ϕ satisfy the same 3-D scalar wave equation

$$P_{xx} + P_{yy} + P_{zz} = v^{-2}(x,y,z)P_{tt,} \tag{2}$$

or

$$\phi_{xx} + \phi_{yy} + \phi_{zz} = v^{-2}(x,y,z)\phi_{tt,} \tag{3}$$

where subscripts denote partial derivatives of P (for equation 2) or of ϕ (for equation 3) with respect to the subscript variable, and v is the acoustic velocity. Implementations of the 3-D

scalar wave equation 2 has previously been presented by Chang and McMechan (1989a, b) and was modified in this study. P is propagated when simulating the acoustic pressure response; ϕ is propagated when simulating the displacement response. Both P and ϕ are scalars so there is no change implied in the wave equation algorithm for the extrapolation of ϕ rather than P; only the physical interpretation of the source wavelet is changed.

To complete this discussion, it should be noted that U may also be computed directly from the gradient of pressure P (cf. Sheriff and Geldart, 1982; Aki and Richards, 1980; Ewing et al., 1957) using

$$\rho U_{tt} = -gradP, \tag{4}$$

where ρ is density. This is equivalent to, but computationally more complicated than, using equation 1. Equation 1, implemented by spatial differencing of values of the propagating ϕ wavefield (eq. 3), are used for all the synthetic examples. Simulating 4-C seismic responses, including pressure (or displacement potential) and partially resolved displacement even for SH and Love waves, may be possible for practical application.

Finite-difference modeling is a remarkably flexible tool that can simulate the seismic response of complex geologic structures (Mufti and Fou, 1989; Mufti, 1989, 1990). The wave-equation based numerical method can account for many types of wave phenomena, e.g., diffraction, interference, and the generation of multiple reflections. The scheme allows lateral and vertical variations in the acoustic velocity but require the density of the medium to be constant. Although this simplification may rule out the generation of shear and surface waves, it is still accurate enough for many important exploration problems. The acoustic approximation of seismic data is a compromising approach compared to a 3-D computation of elastic response.

In our application, the wavefield is pressure and the equation governing its behavior is the acoustic wave equation. The finite speed of sound propagation means that computing the next time value of pressure at a point in the medium cannot involve the values of pressure of large distances away. At each time step, we apply the finite-difference representation of the wave equation to each piece of data (Chang and McMechan, 1989a). The leap-frog scheme (Kreiss and Oliger, 1973) is used to solve for the updated wavefield from wavefields at the previous two time steps. For reasons of stability and accuracy, the time step in our finite-difference simulation is purposely chosen to be small. Practical consideration of simulating a semi-infinite medium on a finite computational grid should be considered by appropriate elimination of boundary reflection. A modified Clayton and Engquist's A_2 boundary conditions (Clayton and Engquist, 1977) are used on the right, left and bottom edges of the model. A stress-free condition (P = 0) is used on the top surface in order to generate the multiple reflection sequence.

3. SYNTHETIC EXAMPLES

Displacement potential and three-component acoustic displacement responses may be computed for all desired recording geometries. The algorithm is demonstrated by simulating data from a surface source recorded on a circular array; a vertical seismic profile and both off-

end and fan shots recorded on a crooked, wide-aperture refraction array. The first two are computed using a faulted anticline model (Fig. 1) and the rest are computed using a fault-bounded basin model (Fig. 4). All the synthetic seismograms shown not only use the time ramp, to compensate spreading loss, but also scale the amplitude with power in order to make some of the later arrivals visible.
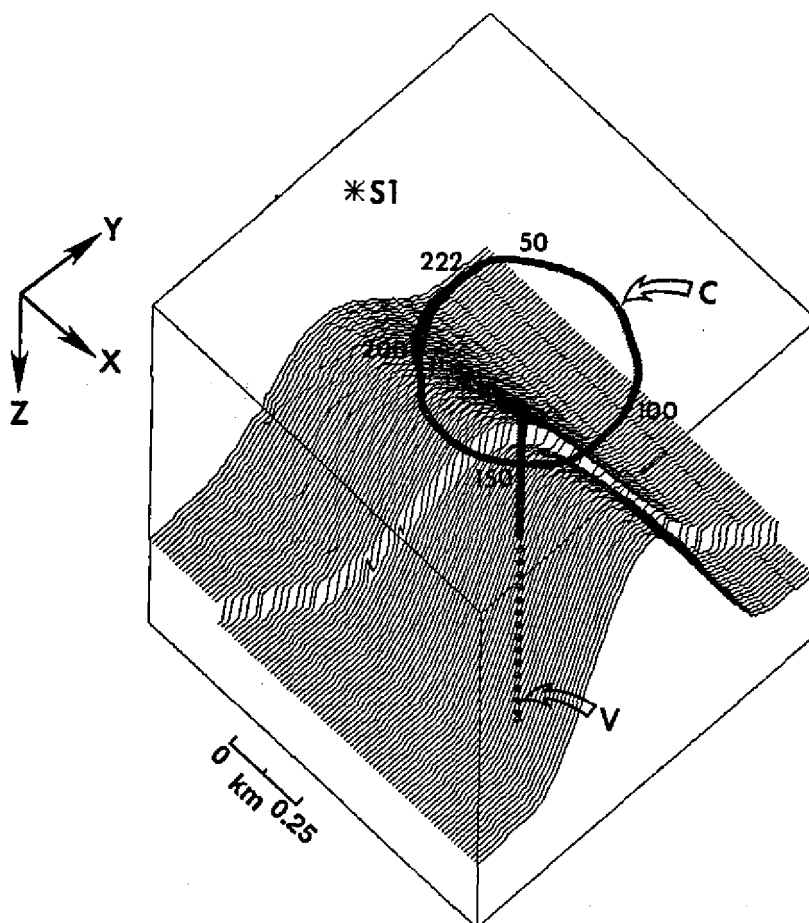

Fig. 1. A faulted anticline model. The velocity above the anticlinal surface is 2.5 km/s; below, 3.5 km/s. The model has dimensions 101 x 101 x 101 points, which corresponds to physical dimensions of 1 km x 1 km x 1 km. Simulated three-component waves from a surface source (S1) recorded on the irregular circular array (C) and the vertical seismic profiles (V) are shown in Figs 2 and 3 respectively. Numbers around C are the same as the trace numbers in Fig. 2. The spacing of the symbols on V is halved below the point of penetration, of the anticlinal surface for clarity, and by the vertical profile. The total geophone station for circle and borehole are 223 and 101 respectively.

3.1 Circular and VSP Gathers Simulation

Figure 1 illustrates the model and source-receiver geometry in our 3-D computation. Source and receivers are located near the surface. The geometry is adopted from actual marine survey geometries (Table 1). The model dimension is 1 km along the x, y, and z directions. The model shows an oblique fault cutting through a plunged folded anticline structure. Both circular-shaped receiver and non-deviated borehole arrays are used to examine their acoustic wavefield responses. The explosive source S1 was located outside the 223-recorder circular array (Fig. 1). The gaussian wavelet is used to represents the apparent source time function. Geographic north is along the y direction.

Synthetic displacement potential and three-component displacement responses are shown in Fig. 2. The acoustic responses include direct arrivals, primary reflections and multiples from free surface and the structure. Observed amplitude variations are related to the separation of responses into orthogonal components as well as their structure. The displacement in the direct arrivals (D) is radially outward from the source, so the amplitude maximum appears in the x-displacement, and the corresponding minimum appears in the y-displacement at traces 28, 117 and 215, which are at the same x-coordinate as the source. Angles of incidence for the later arrivals are modified by the structure, resulting in maximum and null amplitudes in other displacement directions. It is possible to rotate any given three-component data set, by linear combinations, to simulate recording in any other recording direction. Evidence for the fault is seen in all components in the reflections (R) between traces 85 and 155, where there is a time delay of ≈ 30 ms. This energy is reflected from the down-thrown side of the fault. An interesting point to note is that there is apparently a more prominent traveltime shift and a corresponding amplitude and phase change in the free surface multiples. The traveltime shift is more distinct in the y-displacement component mainly due to the orientation of the structure. The main reflections produced by the modeling are used to identify those energy patches corresponding to 3-D propagation effects as seen for the circular and VSP data. Thus, we can see that the structure and the source-receiver geometry play an important role in 3-D modeling. The relationships among source, receiver location and complexity of the subsurface structure will produce different three-component responses.

Table 1. The survey parameters used in figure 1. The kelly bushing (K.B.), the unit at the top of the drill pipe, is used to measure the depth during field survey stage. Both linear and circular walkaway lines were conducted for 3-D survey design and data acquisition.

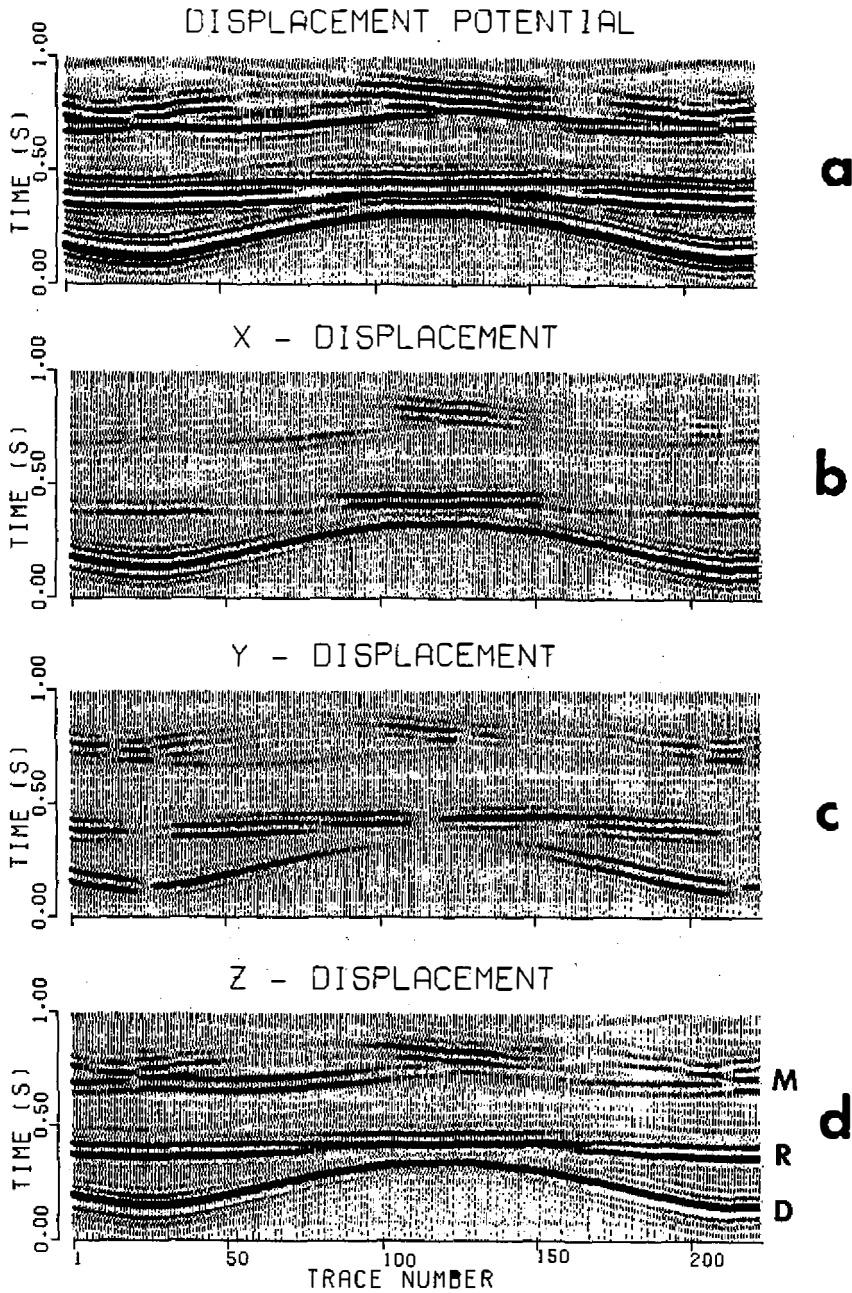|	Short walkaway	Long Walkaway	Circular Walkaway
Geophone Stations	79	11	2
Recording Depth in ft. (km) Below K. B.	7875, - 2025. (2.4 - 0.6)	3100. - 2600. (0.95-0.8)	6000. - 3000. (1.8 - 0.9)
Recording Spacing in ft. (km) below K. B.	75 (0.023)	50 (0.02)	
Source	≈60	≈170	223, 218
Source Spacing in ft. (km)	100 (0.03048)	100 (0.03048)	100 (0.03048)

Fig. 2. Synthetic displacement potential (a), and acoustic displacement response components (b, c, and d) recorded on the circular array C (Fig. 1). Locations of traces are shown in Fig. 1. D is the direct arrival, R is the primary reflection from the anticlinal surface, and M is the first free-surface multiple. High amplitudes are clipped. See discussion in the text.
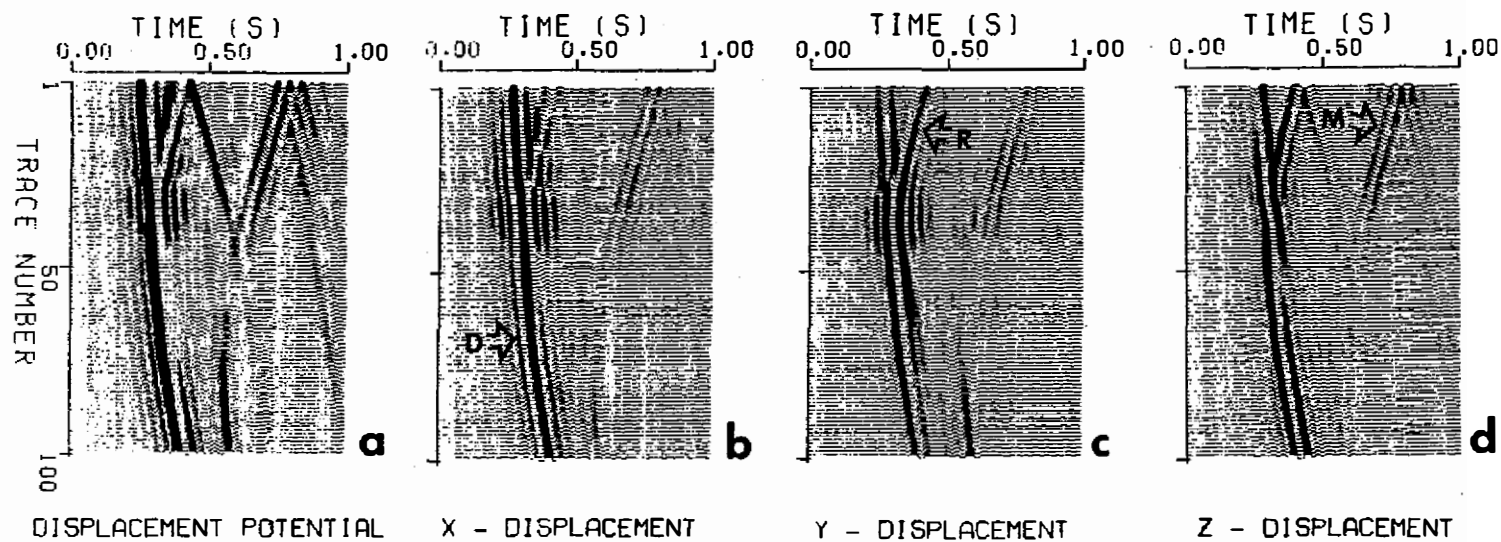
Fig. 3. Synthetic displacement potential (a), and acoustic displacement response components (b, c, and d) recorded on the vertical seismic profile (Fig. 1). Trace separation is 0.01 km. D is the direct arrival, R is the primary reflection from the anticlinal surface, and M is the first free-surface multiple. High amplitudes are clipped. See discussion in the text.

Synthetic displacement potential and three-component displacement responses of the faulted anticline model to source S1 recorded on the 100-recorder vertical seismic profile (Fig. 1) are shown in Fig. 3. These were produced by the same finite-difference calculation that generated the circular array data in Fig. 2. For a single source, synthetic seismograms may be generated simultaneously for all grid points. Downgoing and upcoming waves and their corresponding multiple reflected from the structure boundary are distinguishable in the synthetic 4-C data.

3.2 Wide-angle SH and Love Wave Simulation

For the investigation of large-scale crustal structure, a densely recorded multi-component wide-aperture seismic experiment is necessary and should be conducted using large aperture receiver arrays. The fault-bounded basin model with source S2 located near the end of the 90-
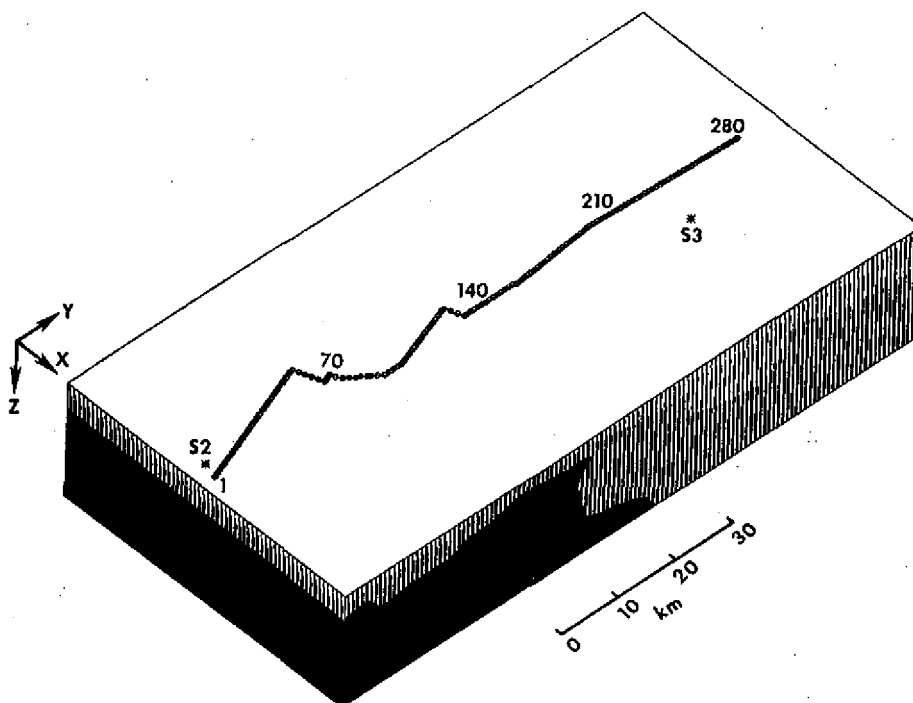

Fig. 4. A fault-bounded basin model. This is similar to the model obtained by Zhu and McMechan (1989) for the interface between the Wichita Uplift and the Anadarko Basin in southwestern Oklahoma; the (high velocity) uplift is on the left and the (low velocity) basin on the right. Velocities are indicated by the 4-level gray scale; velocity values separating gray levels are 3.5, 4.82 and 6.13 km/s. Synthetic seismograms for source S2 and S3 are shown in Fig. 5 and Fig. 6 respectively. Surface receivers are numbered to show the locations of the traces in Figs 5 and 6.

km-long, 281-receiver crooked-line (Fig. 4) is used to simulate SH and Love wave responses from finite-difference computations. Synthetic displacement potential and three-component displacement responses are shown in Fig. 5.

The main difference in seismic response compared to the result from a faulted anticline model (Fig. 1) is that the well-developed SH and Love waves are more prominent due to structural characteristics. The amplitude in the y-displacements is larger than that of the x-displacements because the dominant direction of propagation is nearly parallel to the y-axis
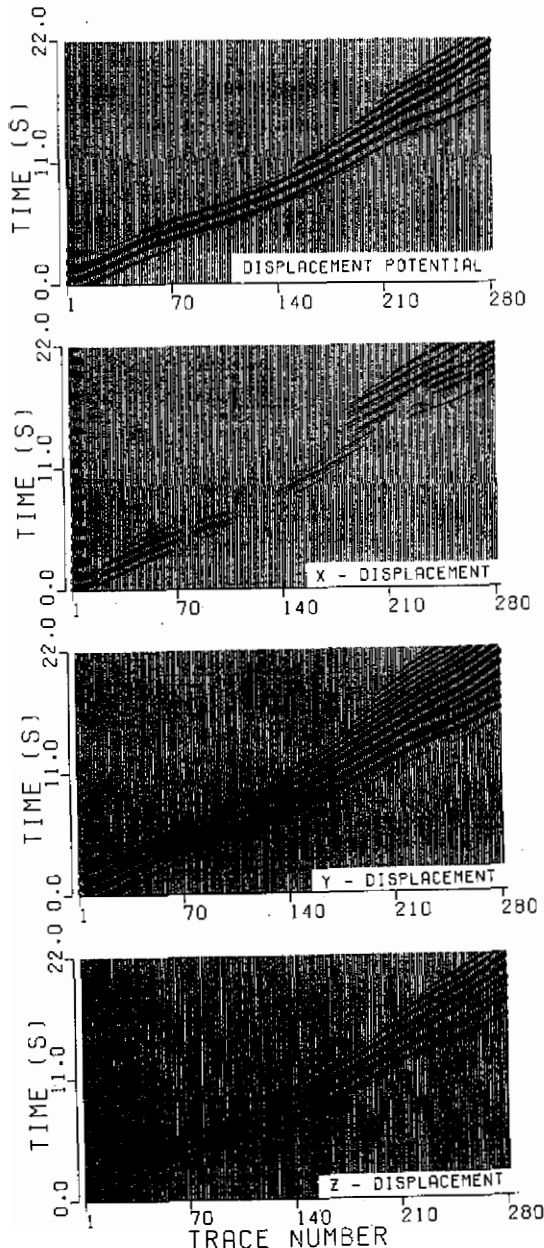
Fig. 5. Synthetic displacement potential (a), and acoustic displacement response components (b, c, and d) for off-end shot S2 on the surface of the fault-bounded basin model (Fig. 4). Locations of source and receivers are shown in Fig. 4. A time-dependent amplitude (ramp) factor increases the relative visibility of the energy at later times; the ramp applied to the x-component increases the amplitude at a rate that is three times that for the other plots. The apparent change of phase velocity near trace 60 is due to a change in the direction of the recording line (Fig. 4).

(Fig. 4). The resonances visible in the first few traces (especially in the x-displacement component) are due to multiples in the thin, surficial low-velocity layer near the source (Fig. 4). The resonances developing in the farther offset traces (>140) are dispersive guided waves in the basin (Fig. 4). Simulating the survey geometry directly *in situ* obviates the need for crooked-line processing, in which sources and receivers are projected onto a 2-D plane.

Synthetic displacement potential and three-component displacement responses of the fault-bounded basin model to off-line source S3 (Fig. 4), are shown in Fig. 6. Reflection R1 is
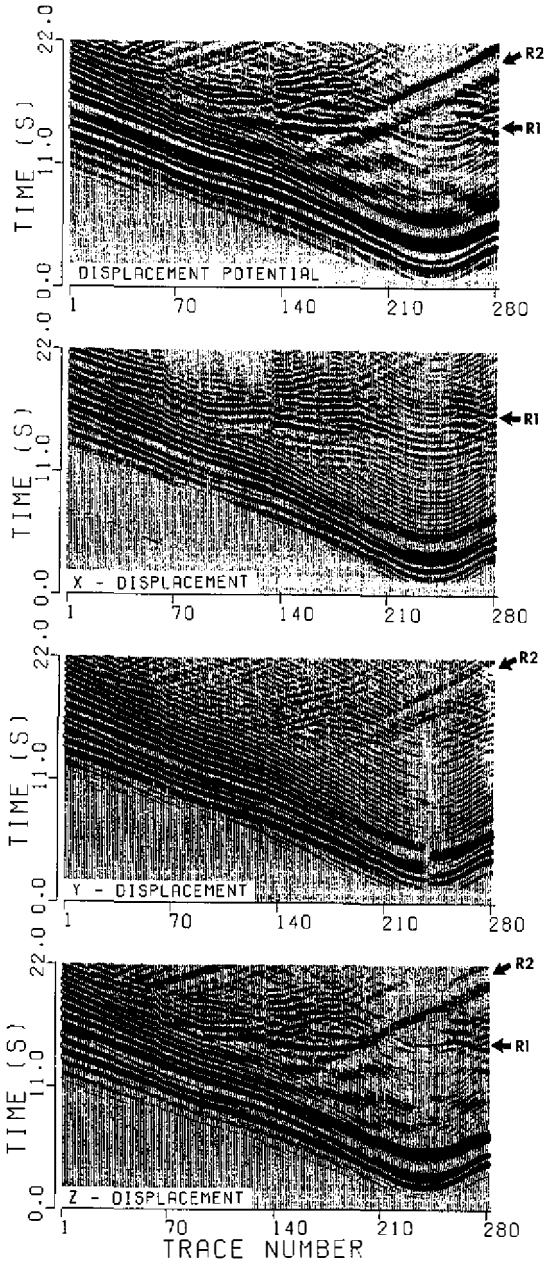

Fig. 6. Synthetic displacement potential (a), and acoustic displacement response components (b, c, and d) for off-line shot S3 on the surface of the fault-bounded basin model (Fig. 4). Location of source and receivers are shown in Fig. 4. A time-dependent amplitude (ramp) factor increases the relative visibility of the energy at later times. Large amplitudes are clipped.

reflected (approximately) from the bottom of the basin structure such that the energy is predominantly in the vertical plane. R2 is an off-line reflection from the high lateral velocity contrast and is propagated predominantly along the y-z plane. Therefore, the R2 component is dominant in the horizontal plane. The source and receiver geometry is another important factor that controls not only the first arrivals but also the later events in the synthetic and field data. In contrast, compared with the nearly in-line shot data in Fig. 5, the off-line source position, the out-of-plane reflection, and the crooked recorder line all require 3-D modeling.

4. DISCUSSION AND CONCLUSION

I present a 3-D finite-difference acoustic computation of 4-C synthetic seismograms for 3-D velocity distributions. The scheme is based on an explicit 3-D second order acoustic finite-difference approximation. The algorithm is demonstrated on different survey geometries, such as circular walkaway and reverse-VSP data for three-dimensionally variable structures. The proposed procedure may provide an alternative approach for 3-D modeling of field data as a complement to full 3-D elastic simulation. Although the compressional and decoupled-SH or Love arrivals are included, the proposed approach does not predict coupled energy such as converted phase in the current implementation. For field data interpretation, an integrated approach including 3-D scalar, partially resolved 3-component displacement and elastic wavefield modeling may be necessary for seismic event identification and subsurface structure discrimination. If necessary, a specific polarization analysis can be used for multi-component multi-offset circular walkaway and VSP data.

It is known that the conventional 2-D algorithm when applied to actual 3-D field recorded data always assumes that the seismic energy is confined within the plane of a 2-D structure profile. From field data records, the transmitted and reflected seismic energy is obtained both from in-plane as well as from out-of-plane propagation effects. The recorded seismic responses are strongly related to subsurface structure and source-receiver geometry. Therefore, 3-D simulation of actual field geometry seismic data is necessary. The major advantage of the current algorithm is its flexibility in modeling diverse source and recorder configurations, e.g., crooked refraction lines and circular arrays. The method has been developed and currently we are applying it to 3-D modeling of marine seismic common-receiver OBS records from offshore eastern Taiwan.

Three-component displacement seismograms may be synthesized by computing orthogonal spatial derivatives of a propagating (scalar) displacement potential wavefield in a 3-D model. The implementation requires the existence of a solution to the 3-D scalar wave equation. The low-order finite-difference method usually requires a relatively large memory to achieve better accuracy; however, the computation is relatively fast. The capability of obtaining low-frequency responses and fast computation is particularly suitable for the synthesis of SH or Love wave wide-angle data. For 2-D seismic applications, the entire data set can be stored in core memory such that computing implementation may not be too difficult. For 3-D applications, the data set may be so large that whole data volume cannot be stored in one memory. However, memory limitation can be alleviated with the advent of computer technol-

ogy. An alternative strategy is the implementation of parallel algorithm (Chen, 1999) on a multi-processor computer.

Two approaches to produce three-component displacement seismograms from an acoustic 3-D finite-difference solution are possible; one is directly from the gradient of the displacement potential, and the other uses the gradient of the pressure distribution. The former is applied here. The same idea would be applicable for ocean bottom cable (OBC) technology (Zachariadis et al., 1986) and vertical receiver arrays (L. Sonneland E. A., 1986) in marine seismic exploration. In terms of application in real marine surveys, the pressure gradient may be measured directly using orthogonal hydrophone arrays. From such measurements, particle displacements may be computed.

Ideally, it would be desirable, especially for land surveys, to consider three-component elastic rather than acoustic displacements so that shear as well as compressional waves would be included. Since the scalar wave equation is equally applicable to SH and acoustic waves (Kelly, 1983), the algorithm presented can be directly applied to compressional (acoustic) seismic waves. The fully-coupled P-SV case requires replacement of the scalar wave equation with the elastic wave equation. Formulations are available and have been implemented for the solution of the 3-D elastic wave equation directly in terms of three-component displacements (cf. Chang and McMechan, 1989a). However, these formulations are approximately three times more expensive than the corresponding scalar computations. The present approach is a compromise that includes only compressional waves, and so is most applicable to the context of marine surveys.

REFERENCES

Aki, K., and P. G. Richards, 1980: Quantitative Seismology, W. F. Freeman and Co., San Francisco, Calif., 932 pp.

Aminzadeh, F., N. Burkhard, T., Kunz, L. Nicoletis, and F. Rocca, 1995: 3-D modeling project: 3rd report, The Leading Edge, Vol. 14, No. 2, 125- 128.

Chang, W. F., and G. A. McMechan, 1989a: Absorbing boundary conditions for 3-D acoustic and elastic finite-difference calculations. *Bull. Seis. Soc. Am.*, **79**, 211-218.

Chang, W. F., and G. A. McMechan, 1989b: 3-D acoustic reverse-time migration. *Geophys. Prosp.*, **37**, 243-256.

Chen, H. W., and G. A. McMechan, 1992: Computation of multi-attribute seismic wavefields by solution of the elastodynamic equations. *Bull. Seism. Soc. Am.*, **82**, 1134 - 1143.

Chen, H. W., and G. A. McMechan, 1993: 3-D physical modeling and pseudo-spectral simu-

lation of seismic common-source data volumes. *Geophysics*, **58**, 121 - 133.

Chen, H. W., 1996: Staggered-grid pseudospectral viscoacoustic wave field simulation in two-dimensional media. *J. Acoust. Soc. of Am.*, **100**, No. 1, 120-131.

Chen, H. W., 1998: Three-dimensional geometrical ray theory and modelling of transmitted seismic energy of data from Nevada Test Site. *Geophys. J. Int.*, **133**, 363-378.

Chen, H. W., 1999: Distributed parallel computing of prestack viscoacoustic pseudospectral modeling, submitted to Geophysics.

Clayton, R., and B. Engquist, 1977: Absorbing boundary conditions for acoustic and elastic wave equations. *Bull. Seism. Soc. Am.*, **67**, 1529-1540.

Ewing, M. W., W. S. Jardetzky, and F. Press, 1957: Elastic Waves in Layered Media: McGraw-Hill, New York, N.Y., 380 pp.

Kelly, K. R., 1983: Numerical study of Love wave propagation. *Geophysics*, **48**, 833-853,

Kreiss, H. O., and J. Oliger, 1972: Comparison of accurate methods for the integration of hyperbolic equations. *Tellus*, **24**, 199-255.

Mufti, I. R., and J. T. Fou, 1989: Application of three-dimensional finite-difference seismic modeling in oil field exploitation and simulation. *Int. J. Imag. Sys. Tech.*, **1**, 28-32.

Mufti, I. R., 1989: Numerical experiments with a salt dome. *Geophysics*, **54**, 1042-1045.

Mufti, I. R., 1990: Large-scale three-dimensional seismic models and their interpretive significance. *Geophysics*, **55**, 1166-1182.

Sheriff, R. E., and L. P. Geldart, 1982: Exploration Seismology. Vol. 1, Cambridge University Press, Cambridge, U. K., 253 pp.

Sonneland L. E. A., 1986: 2-D deghosting using vertical receiver arrays, in Expanded Abstracts, 48th Annual Int. EAEG meeting.

Versteeg, R. J. and G. Grau, 1990: The Marmousi experience, Proceedings of the 1990 EAEG Workshop on practical aspects of seismic data inversion. Eur. Assn. Expl. Geophys.

Zhu, X., and G. A. McMechan, 2-D tomographic imaging of velocities in the Wichita Uplift - Anadarko Basin region of southwestern Oklahoma. *Bull. Seism. Soc. Am.*, **79**, 873-887, 1989.

Zachariadis, R. G., and E. A. Bowden, 1986: Ocean bottom cable: a fixed multichannel sea floor reflection system, in Expanded Abstracts, 56th Annual. SEG meeting, Houston, Tx.